



PREPARATION, CHARACTERIZATION AND MEDICINAL APPLICATION OF CHITOSAN BASED BIOMATERIAL

M. Charumathy, PG & Research Department of Biochemistry, Marudhar Kesari Jain College for Women, Vaniyambadi, Tamil Nadu.

Email: mcharumathy4@gmail.com

Nalini R Uthaman, Department of Applied Sciences, University of Technology and Applied Sciences, Muscat, Sultanate of Oman

Email: nalini.ramachandran@utas.edu.om

R. Saravanan, PG and Research Department of Zoology, Dr Ambedkar Government Arts College, Vyasarpadi, Chennai, Tamil Nadu.

Email: rsaravanan0268@gmail.com

Bharti Ghude Wadekar (B.G. Wadekar), Department of Microbiology (ID), Thakur Shyamanarayan Degree College, Kandivali East, Mumbai, Maharashtra.

Email: bhartiwadekar@tsdcmumbai.in

N. Bhuvana, Department of Chemistry, Jeppiaar Institute of Technology, Chennai, Tamil Nadu.

Email: bhuvana_jerin@yahoo.com

Zoyeb Mohamed Zia, P.G and Research Department of Zoology, The New College (Autonomous), Chennai, Tamil Nadu.

Email: zoyebmdzia@gmail.com

DOI: 10.48047/ecb/2023.12.si4.1608

Abstract

Wastes from the leather industry include chrome shavings, which are rich in type I collagen and can be removed using an alkaline hydrolysis process. Since the generated collagen (Co) has qualities similar to those of the skin's extracellular matrix, it can be employed to speed up the healing of wounds. The linear polysaccharide chitosan (Ch) isolated from shrimp shells has been shown to hasten the development of fibroblasts and increase early phase reactions related to wound and burn healing. Wound dressings containing collagen and chitosan, a muco-adhesive fiber-producing natural polymer that offers an appealing alternative to traditional sustained medication release systems, are in the works. However, silver nanoparticles (AgNp) generated from *Hibiscus rosa-sinensis* are utilized in conjunction

with collagen and chitosan to create a wound dressing material. Moisture content, porosity measurement, water absorption, and mechanical properties were among the tests performed on the wound dressing materials (Co-Ch-AgNp). FTIR was used to examine the functional groups. SEM analysis of the surface morphology.

Keywords: Chitosan, Silver nanoparticles, wound dressing materials and Collagen.

Introduction

Scaffolds in tissue engineering and bone engineering can be made from a wide range of materials. The content and structure of biodegradable polymers can be tailored to meet a variety of applications; furthermore, they are engineered to break down when new tissues grow, leaving no foreign material behind. This scaffold material should be able to recreate the in vivo microenvironment, which is primarily provided by the extracellular matrix, so that cells can attach, proliferate, and differentiate into functionally and structurally appropriate tissue for the specific body location into which it is placed. Scaffolds employed in this way should integrate biophysical, biomechanical, and pharmacological signals that promote cell proliferation, differentiation, maintenance, and function, and that can serve as templates for tissue regeneration. In the case of extensive third-degree burns, skin restoration becomes a critical area of tissue engineering. Several natural polymers wound dressings are presented as biomaterials in this context only. Natural polymers induce and stimulate the wound healing process, playing a role in tissue repair and skin renewal [1-5].

These are typically made of a polymeric network that contains water at a concentration of 99 percent or greater. One typical approach in tissue engineering is to use three-dimensional polymeric scaffolds for cell targeting. Biocompatible and biodegradable natural/synthetic polymers have been the subject of extensive research in recent years, leading to the creation of innovative forms of wound dressings with wide-ranging biomedical uses, especially in the field of regenerative medicine. There is a total of five phases to the wound healing process, each of which involves its own set of biochemical and cellular mechanisms. Blood clotting, inflammation, migration, cell division, and finally, differentiation is the five stages listed. The rate at which a wound heals can be affected by the use of appropriate materials. Studies have revealed that including neem extract into collagen sheets improves the biostability of the biocomposite film and affects its ability to scavenge nitric oxide. Symptoms of inflammation include redness, warmth, swelling, edema, discomfort, and dysfunction. The blood vessels in the wound bed will constrict and a clot will form whenever a wound is sustained. Blood

arteries under the wound enlarge during hemostasis, allowing antigen-specific T lymphocytes, cytokines, chemokines, growth factors, enzymes, and nutrients to reach the injured area. During the proliferative phase, a process termed "angiogenesis" rebuilds the wound by forming a new tissue composed of collagen and extracellular matrix within which a network of blood vessels develops. The process by which the epidermis, the skin's outermost layer, returns to the surface after a wound has healed, is called epithelialization. Collagen extracted from chromium shavings saturated with neem extract makes for an excellent wound dressing since it possesses both the mechanical and biological qualities necessary for its use [6-9].

It was found that collagen biocomposite could scavenge nitric oxide after being modified with neem extract. Therefore, it has the potential to be used as a diabetic wound dressing. The collagen matrix not only aids in cell adhesion and proliferation, but also acts as a support matrix for the controlled release of extracts. The anti-microbial and anti-oxidant characteristics of phenolic components like tannin and flavonoid content contained in teak leaf have accelerated the healing process. The epithelization time is shortened by the artificial sheet that combines the benefits of collagen and teak leaf extract. Commonly known as "shoe-flower," or *Hibiscus rosa-sinensis*, this plant is used medicinally for its anti-inflammatory and antioxidant properties. Silver nanoparticles isolated from *Hibiscus rosa-sinensis* have been shown to hasten re-epithelization and fibroblast differentiation, as well as alter the modulation of fibrogenic cytokines. To improve wound healing activity, a biomaterial was developed using natural polymers mixed with silver nanoparticles and used as a wound dressing. The biomaterial was shown to be nontoxic, biodegradable, and biocompatible. Biomaterials for use in wound healing may be prepared from a variety of materials, including silver nanoparticles and natural biodegradable polymers like collagen and chitosan [10-13].

More than 30% of a human's body is made up of collagen, with type I collagen being the most prevalent in skin and connective tissue. Bone is mostly composed of collagen and hydroxyapatite. In terms of volume, it accounts for 32% of bone and 89% of the organic matrix. The three most frequent kinds of collagen in humans are types I, II, and III. Collagen/hyaluronan/beta glucan was found to be non-toxic and biocompatible with cultivated cells in an in vitro study. It had a beneficial effect on ECM production. Different amounts of NaCl did not affect the efficacy of nanocomposite collagen coatings. Chitosan is a

polysaccharide made up of (1-4) connected 2- acetamido- 2- deoxy- - D-glucose and is the second most abundant natural polysaccharide on Earth, behind cellulose. Chitosan is obtained by treating shrimp shells with alkali and acid. Wounds and burns are treated with it because of its hemostatic effect. Increased fibroblast production and wound healing phases are both facilitated by chitosan. Silver nanoparticles have been employed in silver-based dressings and silver-coated medical devices due to their potential efficacy as an antibacterial agent. Wound dressings made of silver-loaded chitosan nanoparticles have been employed in tissue engineering. Burn, open wound, and chronic ulcer infections have benefited greatly from their use. By encouraging keratinocytes to proliferate and migrate, they speed up the healing process. By stimulating wound contraction, they contribute to the differentiation of fibroblasts into myofibroblasts. Better fibril alignments in restored skin that closely resembles native skin are the result of using silver nanoparticles with enhanced tensile characteristics. Biocomposite sheet is one of the best materials for making 'moist healing' wound dressings due to the unique properties of collagen, chitosan, and silver nanoparticles. Drug delivery systems and cell encapsulation are only two of the many pharmaceutical and biomedical applications for biocomposite sheets due to their biodegradability and biocompatibility [15-20].

Nanoparticles were generated from *Hibiscus rosa-sinensis* utilizing poly ethylene glycol as a crosslinker and incorporated into a composite made from tannery waste collagen, prawn shell chitosan, and tannery waste chitosan. Physical and chemical characteristics, including ash and moisture levels, porosity and water absorption tests, tensile strength and elongation at break, and FTIR analyses, were determined for the biocomposite sheet after it was manufactured [21].

Materials and Methods

Collagen extraction from chrome containing leather waste (CCLW)

It was at the Central Leather Research Institute in Adyar, Chennai that we obtained the sample of leather scrap containing chrome. After soaking 50 grams of the sample in 5% NaOH and then treating it with 10-15 milliliters of strong sulphuric acid to dechrome the leather, the resulting collagen was bleached with 10 milliliters of hydrogen peroxide until it was colorless and then stored at 4 degrees Celsius and twenty-five percent relative humidity.

Extraction of chitosan from shrimp shells

After being obtained at the Chintadripet market, the shrimp shells were treated as follows.

Demineralization

The shells of the shrimp were demineralized with HCl at a concentration four times that of 1%. After soaking for 24 hours, the samples were mineral-free.

After demineralization, 50 mL of a 2% NaOH solution was used to break down the albumen into water-soluble amino acids in the shrimp shell samples for an hour. De-ionized water was used to flush away any lingering chitin. Deacetylation was used to transform the chitin into the final product, chitosan.

Deacetylation

To deacetylate, we boiled the substance at 100 degrees Celsius for two hours after adding 50 percent NaOH. The samples were then chilled for 30 minutes at room temperature under the hood. In order to keep the chitosan-containing solids, the samples are continuously washed with the 50% NaOH and filtered. The samples were subsequently dried in an oven at 110°C for 6 hours after being left uncovered.

Determination of Degree of Deacetylation for Chitosan

Degree of Deacetylation determined using the equation proposed by as given as,

$$DD (\%) = 100 - [(A_{1655}/A_{3450}) \times 100/1.33]$$

where, A_{1655} – Amide-1 measure of N-acetyl group. A_{3450} – Hydroxyl bond 1.33 – Value of ratio (A_{1655}/A_{3450}) for fully acetylated chitosan [35].

Ash content

The sample weight was 1 g, and it was placed in a crucible with a lid and heated in a muffle furnace at $575 \pm 10^\circ\text{C}$ for 6 hours. When it reached room temperature, the crucible was taken out of the furnace. This process was done 30 times until a stable weight was achieved. The formula used to get the ash percentage is as follows:

$$\text{Ash } (\%) = \text{Wt. of ash (g)}/\text{Wt of sample (g)} \times 100.$$

Moisture content

The samples were dried to constant weight in oven at 105°C and moisture content was

calculated with the formula, Moisture (%) = $(W_1 - W_2 / W_1) * 100$

Where W_1 = weight (g) of the sample before drying, W_2 = weight (g) of the sample after drying.

displacement liquid because of its easy penetration through the pores of the biocomposites and which will not induce shrinking or swelling as a non-solvent of the polymers.

A known weight (W) of the biocomposite was immersed in a graduated cylinder containing a known volume (V_1) of ethanol. The biocomposites sheets were kept in ethanol for 5 min.

The process was repeated until the air bubble stops. The total volume of ethanol and the ethanol impregnated biocomposites was recorded as V_2 .

The difference in the volume was calculated by $(V_2 - V_1)$. The biocomposite impregnated with ethanol was removed from the cylinder, and V_3 is the residual ethanol volume. Thus, total volume of the biocomposite was calculated by

$$V = (V_2 - V_1) + (V_1 - V_3)$$

Porosity of the biocomposite was obtained with,

$$\epsilon = (V_1 - V_3) / (V_2 - V_3)$$

Silver nanoparticles synthesis

The shoe flower (*Hibiscus rosa-sinensis*) was picked, cleaned in distilled water, and dried in the sun. The petals were sliced thinly and cooked in a pot of distilled water over a stovetop burner. After filtering, a 1:10 mixture of silver nitrate solution (1 mM) was added. The beaker was then left out in the sun to fade from a pale crimson to a dark brown. Absorbance measurements were made from 300 to 600 nm. The solution was centrifuged at 10,000 rpm, and then the pellet was re-dispersed in acetone to remove any impurities. The solution was dried, and the resulting nanoparticles were kept at 40 degrees until additional study was possible.

Biocomposite sheet formation

Sheets of Co-Ch-AgNPs were produced, cross-linked with PEG, and then kept at room temperature for later study.

Water Absorption Studies

Swelling tiny sections of each biocomposite of known weight in room-temperature distilled water allowed us to calculate the biocomposite sheets' ability to absorb water. After blotting the biocomposite sheets with filter paper to remove excess, their weight was observed at 1, 2, 3, and 24 hours. Using the method, we were able to determine the percentage of time that the biocomposite sheets would take to absorb water.

$$\text{Water Absorption} = (W_s - W_o) / W_s * 100$$

Where W_s - the weight of the biocomposite (moist) at given time, W_o - the initial weight of the biocomposite.

Porosity Measurement

The porosity of a biocomposite sheet was measured using ethanol and the liquid displacement method of FTIR spectroscopy. Functional groups in the produced biocomposites were identified using Fourier transform infrared spectroscopy. Nicolet 360 Fourier Transform Infrared (FTIR) spectroscopy was used to obtain the spectra, with the frequency range being 4000-500 cm^{-1} .

SEM Analysis

Gold was sputtered onto the prepared biocomposite films to a thickness of 500x108 nm using a SC7640 sputter coater (Quorum Technologies, Newhaven, UK) at 25 °C + 1 °C, 0.1 Torr of pressure, 1-2 kilovolts, and 50 milliamperes. SEM analysis at 20kV revealed interesting details about the shape of the coated sample's surface.

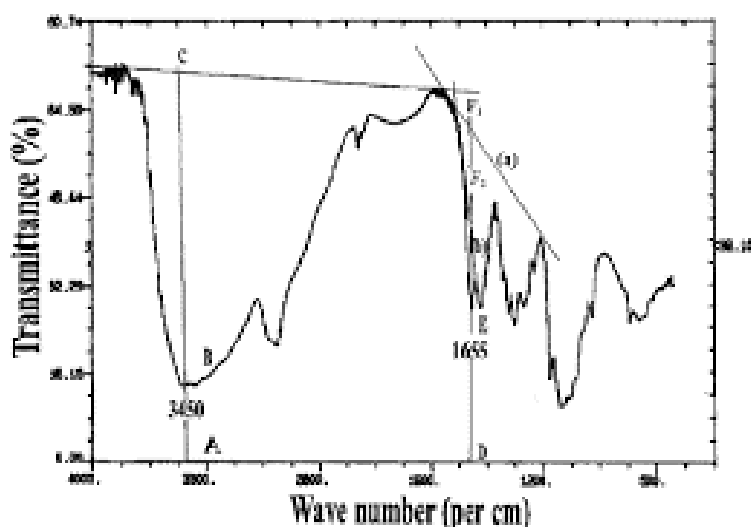
RESULTS AND DISCUSSION

In spite of significant sample loss due to alkali and acid treatments, collagen extraction from chrome-containing leather scraps resulted in a 14% yield. The demineralization technique was used to extract chitosan, and the yield was 28.6 percent. Chitosan's yield and pH drop from 7.8 to 7.0 correspond with the degree of deacetylation. Collagen and chitosan were kept at 4 degrees centigrade until further use.

Table 1: Physicochemical properties of collagen and chitosan

Properties	Collagen	Chitosa n
Ash content	38.57±0.31	3.03±0.20
Moisture content	85.9±.42	2.17±0.75
Yield (%)	14 ±0.11	28.6 ±.023
DDA %		64.48

Determination of Degree of Deacetylation

**Figure 1:** FTIR for calculating Degree of Deacetylation of chitosan

Metal cations are particularly attracted to chitin and chitosan. One of the best adsorbents found in nature, chitosan has a great capacity for absorbing heavy metals cations. Metal cations including copper, mercury, cadmium, iron, nickel, zinc, lead, and silver are all absorbed by it [22-25]]. The degree of deacetylation has a significant effect on the capacity for metal adsorption. However, maxima were seen at around 50% deacetylation in samples obtained by deacetylation in homogeneous solutions; this corresponds to the degree of

deacetylation of the water-soluble chitin. Here is a formula for determining the level of deacetylation:

$$DD (\%) = 100 - [(1629.375 / 3448.629) \times 100 / 1.33] = 64.48 \%$$

Where, 1.33 is the value of ratio A1655/A3450 for fully N- acetylated chitosan. By calculating with the above formula, the degree of deacetylation was found to be 0.64 for the extracted chitosan (Fig.1).

Silver nanoparticles synthesis

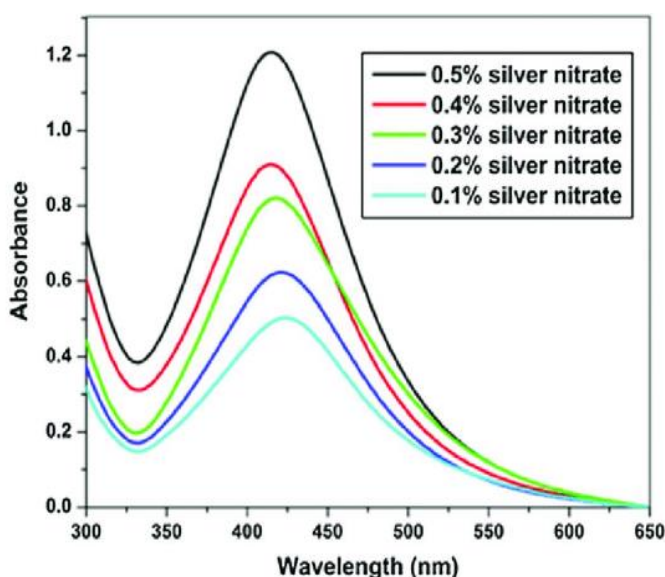


Figure 2: UV absorbance for silver nanoparticles

At ambient conditions, UV-visible absorption spectra were obtained. Between 300 and 600 nm, an optical density reading was taken. The adsorption peak of the produced silver nanoparticles from *Hibiscus rosa-sinensis* occurs at 432 nm (Fig. 2). Nanoparticles created by biological synthesis are typically between 400 and 450 nm¹³ in size.

Table 2: Antibacterial Properties of Collagen, chitosan and silver nano particles

Collagen (w/v %)	Chitosan (w/v %)	AgNP'S (mg)	Antibacterial test
5	20	1	No zone formed

5	20	2	No zone formed
5	20	3	No zone formed
5	20	4	Zone formation (1.5mm)
5	20	5	Zone formation (15mm)

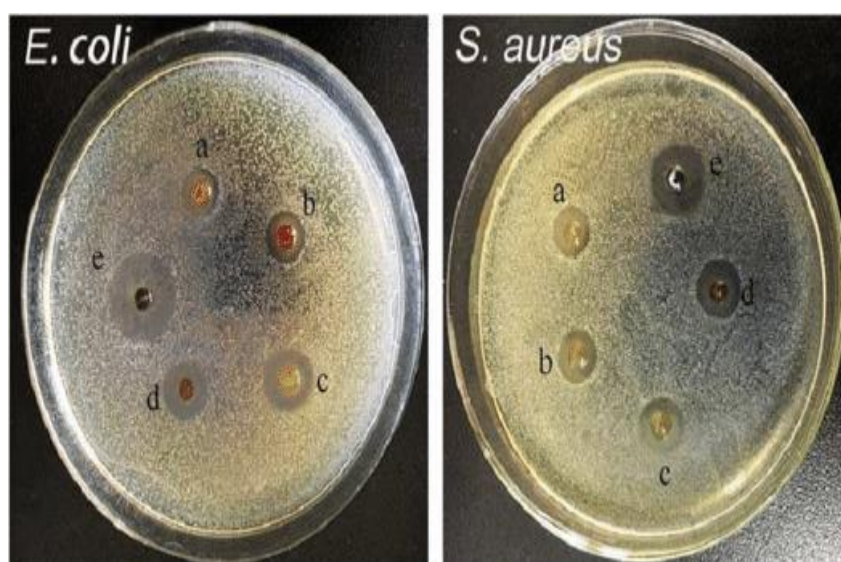
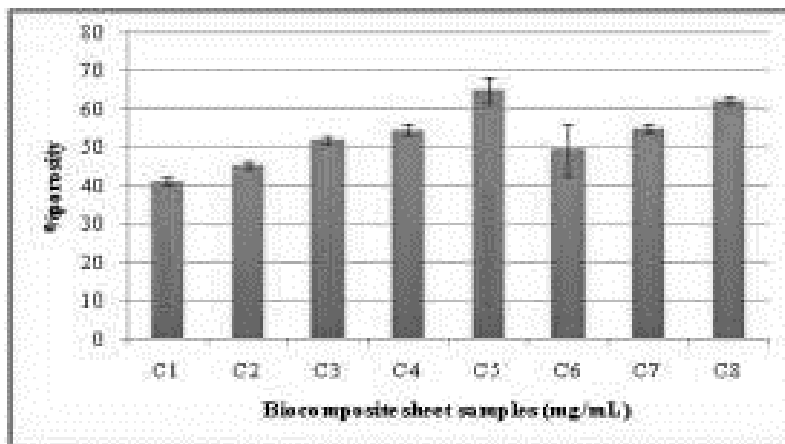
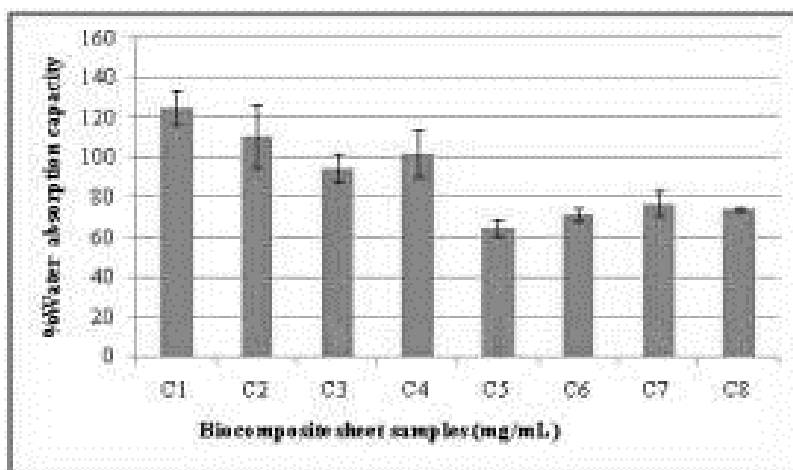


Figure 3: Zone of inhibition of Chitosan, Collagen and AgNPS in petri plates with cultures of *E.Coli* and *Staphylococcus aureus*

Many researchers in the fields of microbiology and science are currently struggling to combat biofouling. Until recently, many different antifouling agents were utilized, including chlorine, antibiotics, etc., but chemicals had hazardous side-effects on humans and bacteria gradually gained resistance to antibiotics [26-29]. Both free silver nanoparticles and those embedded in a polymer matrix have potent antibacterial action. Table 2 shows that when the concentration of silver nanoparticles in biocomposite film increases, so does its antibacterial impact. Figure 3 shows that silver nanoparticles are just as efficient against *E. coli* and *Staphylococcus aureus* when used in disc-shaped petri plates.

Porosity study of biocomposite sheets**Figure 4:** Porosity studies for biocomposite sheet ($p < 0.05$)

Cell attachment and migration in wound healing³⁵ are greatly aided by the pore size, surface area, and porosity of bio composites sheets. All of the materials' porosity was determined to be between 40% and 65% using the liquid displacement method (Figure 4).

Water absorption studies**Figure 5:** Water absorption studies for biocomposite sheet ($p < 0.05$)

For wound healing, the biocomposite sheets must be able to absorb a lot of water without losing their shape. The created bio composites were tested for their ability to absorb water (Figure 5), and the results reveal that all of the bio composites absorb more than 100% of the water used in the test, making them appropriate for use on wounds. Furthermore, all of the bio composites maintained their original shape during the duration of the test, which is

impressive. As can be seen in the graph, the combination of collagen, chitosan, and silver nanoparticles (1:4:1) results in biocomposite sheet with superior mechanical capabilities compared to either collagen or chitosan alone. The tensile strength of a wound dressing is crucial for its portability. The percentage elongation of the Collagen-Chitosan-Silver nano particles combination is found to be mild, making it an appropriate wound dressing material. Figure 6 shows that the biocomposites made from chitosan, collagen, and silver nanoparticles are strong enough to be used as wound dressings.

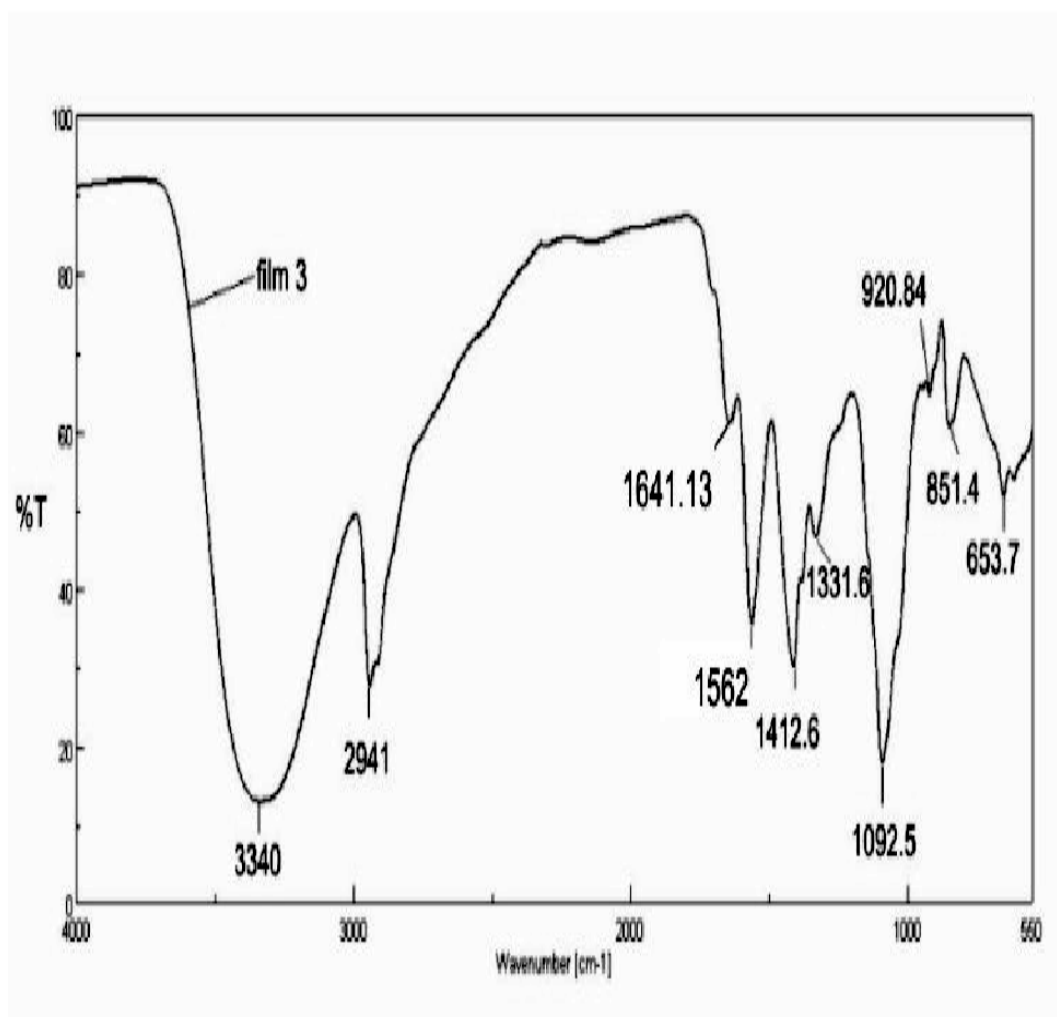


Figure 7: FTIR spectra for extracted chitosan

The characteristics peaks of extracted chitosan was observed from the Fig.7 and the functional properties are explained in the below table. The following absorption bands, 2361.37, 2361.34 cm representing C-N

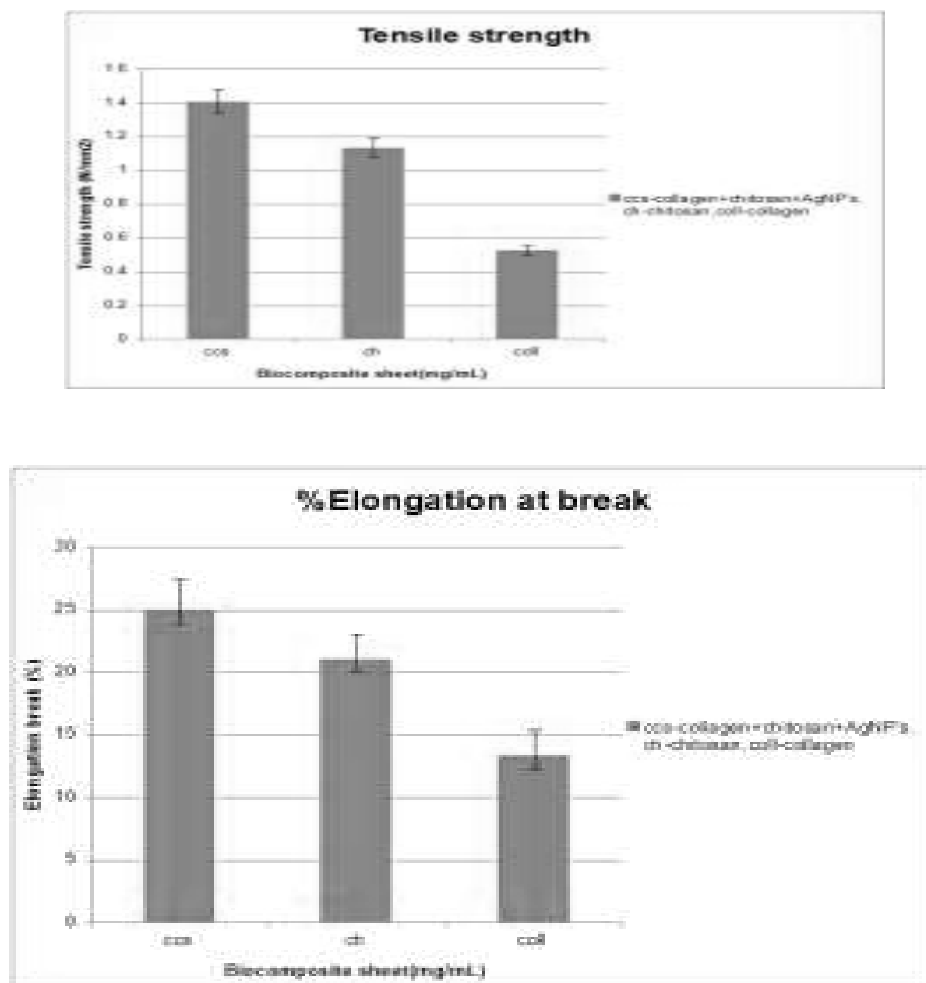
Tensile Strength

Figure 6: Biocomposites' tensile strength and elongation at break when cross-linked with 0.5 mL of polyethylene glycol. ($p < 0.05$) Amide I band at 1629.37 cm^{-1} , acetyl group C-O stretch at 1073.73 cm^{-1} , and amide II band at 1561.21 cm^{-1} all indicate stretching in asymmetric band regions. Then, at 1073.52 cm^{-1} , we get the bridge C-O stretch associated with skeletal vibration. At 2926.37 cm^{-1} , we have symmetric CH₃ stretching.

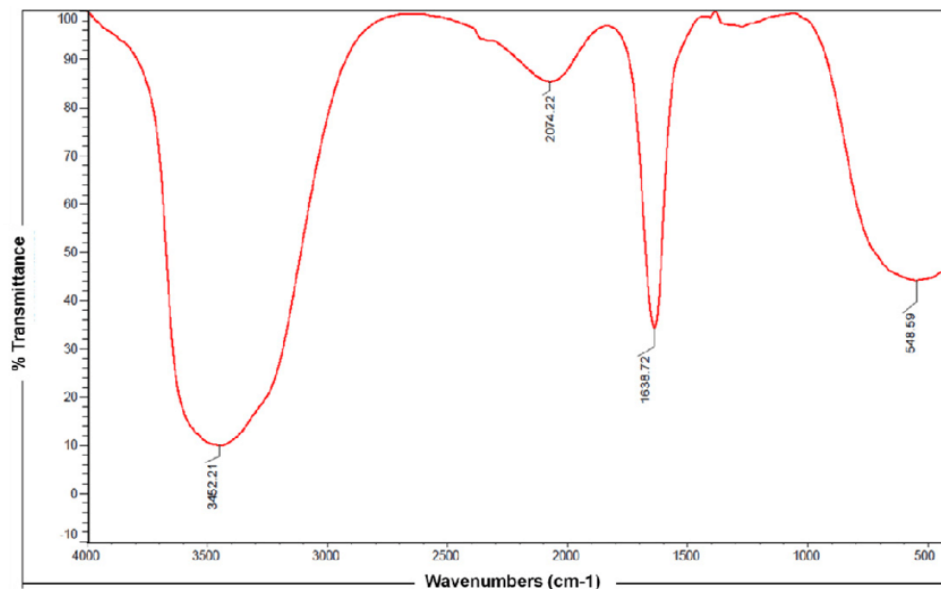


Figure 8: FTIR spectra for silver nanoparticles

The FTIR spectra of silver nanoparticles are shown in Fig. 8. The flower extract was analyzed by Fourier transform infrared spectroscopy (FT-IR) to determine the biomolecules responsible for reducing, stabilizing, and capping the bio reduced silver nanoparticles. The results showed that the carbonyl groups from the aminoacids residues and from the proteins extracts of the flower had a strong ability to bind metal, suggesting that the proteins could possibly form the layer covering the metal nanoparticles and prevent agglomeration, stabilizing the FTIR analysis of artificial AgNPs, a crude extract of *H. sinensis* petals, and a silver nitrate salt. Strong bands corresponding to O-H stretching, H-C-H asymmetric stretching, C-N stretching, C=C symmetric stretching, N-O bending, and C-O stretching were seen in the synthesized AgNPs at 3791.14, 3454.67, 2025.5, 1641.61, 1444.03, 1103.62, and 617 cm⁻¹. The presence of carboxyl and amide groups proves that the nanoparticles were biofabricated through the action of proteins or phytochemicals, serving as a hallmark marker for proteins. Results from Fourier transform infrared spectroscopy (FTIR) show that the presence of chitosan in the produced sheet³⁴, with amide peaks at 1643.27cm⁻¹, 1567.3cm⁻¹, and 1321.05 cm⁻¹, is definitive. The presence of collagen in the produced sheets can be verified by looking for the protein's three distinctive amide peaks. Amide peaks at 1649 cm⁻¹, 1555 cm⁻¹, and 1242 cm⁻¹ were obtained in the FTIR data of collagen composites. Collagen extract was successfully incorporated into the combination sheet, as evidenced by a minor shift in the amide peaks of the collagen, chitosan, and silver nanoparticles biosheet, which was not present in the extraction of chitosan and silver nanoparticles.

SEM Analysis

SEM images of collagen-chitosan (Co-Ch), silver nanoparticles (AgNP), and collagen-chitosan-AgNP (Figs.6, 7, and 8) are shown. Nanostructures of AgNP are easily discernible, as are the crystalline and fibrous structures shown in images of collagen and chitosan. Co-Ch-AgNP composites with uniformly dispersed silver nanoparticles are shown in Fig. 7.

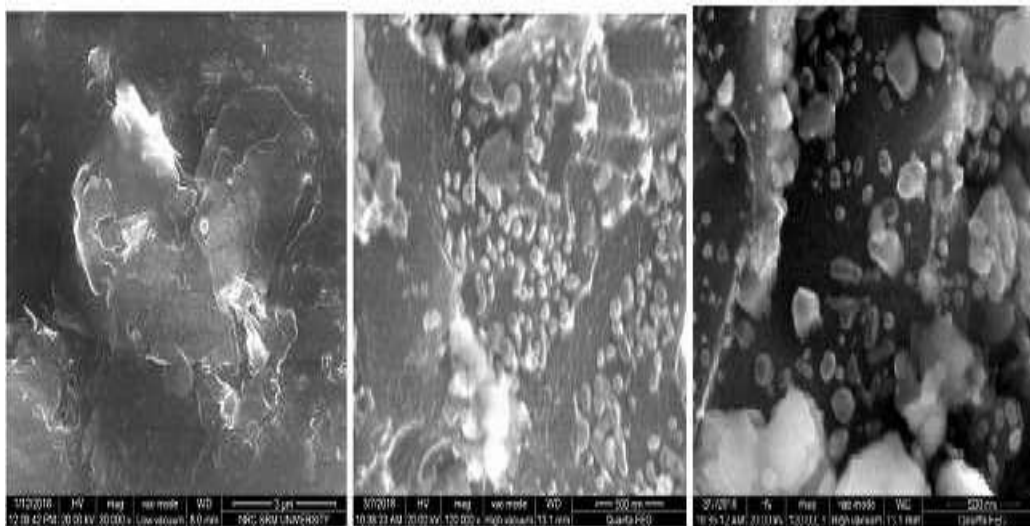


Figure 10. SEM image of Co-Ch

Figure 11. SEM image of AgNP

Figure 12. SEM image of Co-Ch-AgNP

When compared to pure chitosan and collagen films, the composite film made from the three materials proved to be superior. Collagen films have been used as wound dressings, however their low mechanical strength and rapid breakdown rate limit their scope of application. The chitosan provided the film with durability and adaptability. The use of silver nanoparticles boosts its antibacterial action. According to the results, the green AgNPs produced from the *Hibiscus rosa-sinensis* petal extract possessed an efficient antibacterial action against the four pathogenic microorganisms. The Co/Ch//AgNP bio composite films are more malleable than those made from pure collagen and chitosan, and they are also uniform and free of macroscopic flaws [30-34].

Conclusion

Waste from the leather industry is one of the biggest threats to the environment. Chitosan and collagen derived from discarded shrimp shells and chrome shavings, respectively, serve to lessen environmental pollution. Collagen and chitosan were added to isolated silver nanoparticles from *Hibiscus rosa-sinensis*. To test the mechanical strength and other physicochemical parameters of the bicomposite sheets, different stoichiometric ratios were

used to create the sheets. According to the characterization experiments, the generated biocomposite wound dressing sheets have a greater than 100% water absorption capacity and maintain their shape during the healing process. The biocomposite sheets' porosity, as determined by the liquid displacement method, was found to be greater than 60%. The biocomposite sheet is suitable for further use in *in vitro* studies on wound healing due to its strong mechanical and antibacterial properties.

References

1. Huang S, Fu X. Naturally derived materials-based cell and drug delivery systems in skin regeneration. *Journal of Controlled Release*, 142(2), 2010, 149-59.
2. Chandran S, Amritha TS, Rajalekshmi G, Pandima Devi M, Potential wound healing materials from the natural polymers-A review. *Int J Pharm Bio Sci*, 6(3)(B), 2015, 1365-1389.
3. Dai T, Tanaka M, Huang YY, Hamblin MR, Chitosan preparations for wounds and burns: antimicrobial and wound-healing effects. *Expert review of anti-infective therapy*, 9(7), 2011, 857-879.
4. Rathinamoorthy R, Sasikala L, Polysaccharide fibers in wound management. *International Journal of Pharmacy and Pharmaceutical Sciences*, 3(3), 2011, 38-44.
5. Chandran, Amritha TS, Rajalakshmy G, Devi M, A preliminary *in vitro* study on the bovine collagen film incorporated with *Azadirachta indica* plant extract as a potential wound dressing material, *International Journal of PharmTech Research*, 8(6), 2015, 248-257.
6. Shankar M, Ramesh B, Kumar D, Babu M, Wound healing and its importance- a review. *Der pharmacologiasinica*, 1(1), 2014, 24-30.
7. Diegelmann R.F., Evans M.C. Wound healing: an overview of acute, fibrotic and delayed healing. *Front Bioscience*, 9(1), 2004, 283-289.
8. Chandran S, Amritha TS, Rajalakshmy G, Pandima Devi M, Collagen – *Azadirachta indica* (Neem) Leaves Extract Hybrid Film as a Novel Wound Dressing: *In vitro* Studies. *Int. J. Pharm. Sci. Rev. Res.*, 32(2), 2015, 193-199.
9. Amritha, Pandima Devi M, *In vitro* studies on the wound dressing prepared using collagen and Teak leaves (*Tectona randis*). *Journal of Pharmacy Research*, 10(2), 2016, 90-98.

10. Divya MJ, Sowmia C, Dhanya KP, Joona K, Screening of antioxidant, anticancer activity and phytochemicals in methanolic extract of *Hibiscus rosa-sinensis* leaf extract, Research Journal of Pharmaceutical, Biological and Chemical Sciences, 4(2), 2013, 1308-1316.
11. Shabana S, Muzammil MS, Parsana S, Silver nano scaffold formation by flowers of *Hibiscus rosa-sinensis*. International Journal of Herbal Medicine, 1(2), 2013, 169- 174.
12. Thomas, V, Yallapu M, Sreedhar B, Bajpai SK, Fabrication, characterization of chitosan/nano-silver film and its potential antibacterial application, Journal of Biomaterials Science. Polymer Edition, 20(14), 2009, 2129-2144.
13. Danisovic L, Novakova ZV, Bohac M, Bakos D, Vojtassak J. *In vitro* testing of modified collagen/hyaluronan/beta-glucan scaffold. OnLine Journal of Biological Sciences, 13(2), 2013, 40-45.
14. Ma L, Gao C, Mao Z, Zhou J, Shen J, Hu X, Han C. Collagen/chitosan porous scaffolds with improved biostability for skin tissue engineering. Biomaterials, 24(26), 2003, 4833-4841.
15. Khor E, Lim LY, Implantable applications of chitin and chitosan. Biomaterials, 24(13), 2013, 2339-2349.
16. Paul W, Sharma CP, Chitosan and alginate wound dressings: A short review. Trends in Biomaterials & Artificial Organs, 18(1), 2004, 18-23.
17. Mishra M, Kumar H, Tripathi K, Diabetic delayed wound healing and the role of silver nanoparticles. Dig J Nanomater Bios, 3(2), 2008, 49-54.
18. Azuma K, Izumi R, Osaki T, Ifuku S, Morimoto M, Saimoto H, Okamoto Y, Chitin, Chitosan, and Its Derivatives for Wound Healing: Old and New Materials. Journal of functional biomaterials, 6(1), 2015, 104-142.
19. Liu X, Lee PY, Ho CM, Lui VC, Chen Y, Che CM, Wong KK, Silver nanoparticles mediate differential responses in keratinocytes and fibroblasts during skin wound healing. ChemMedChem., 5(3), 2010, 468-475.
20. Kwan KH, Liu X, To MK, Yeung KW, Ho CM, Wong KK, Modulation of collagen alignment by silver nanoparticles results in better mechanical properties in wound healing. Nanomedicine: Nanotechnology, Biology and Medicine, 7(4), 2011, 497-504.

21. Kato Y, Onishi H, Machida Y, Application of chitin and chitosan derivatives in the pharmaceutical field. *Current Pharmaceutical Biotechnology*, 4(5), 2003, 303–309.
22. Deepachitra R, Ramnath V, Sastry, TP, Graphene oxide incorporated collagen-fibrin biofilm as a wound dressing material. *Royal Society of Chemistry Advances*, 4(107), 2014, 62717-62727.
23. Trung TS, Han WW, Qui NT, Ng CH, Stevens WF, Functional characteristics of shrimp chitosan and its membranes as affected by the degree of deacetylation. *Bioresource Technology*, 97(4), 2006, 659-63.
24. Huang M, Khor E, Lim LY, Uptake and cytotoxicity of chitosan molecules and nanoparticles: effects of molecular weight and degree of deacetylation. *Pharmaceutical Research*, 21(2), 2004, 344-353.
25. Muzzarelli RAA, Rochetti R, Determination of the degree of deacetylation of chitosan by first derivative ultraviolet spectrophotometry, *Journal of Carbohydrates and Polymers*, 5(2), 1985, 461-72.
26. Domszy JG, Roberts GAF, Evaluation of infrared spectroscopic techniques for analyzing chitosan. *Die Makromolekulare Chemi*, 186(8), 1985, 1671-1677.
27. Rao KP, Joseph KT, Naydamma Y, grafting of vinyl monomers on to modified collagen by Ceric ion-studies on grafting site, *Leather Sci*, 16, 1969, 401-408.
28. Zhang R, Ma PX, Poly (α -hydroxyl acids)/hydroxyapatite porous composites for bone tissue engineering: Preparation and morphology, *J. Biomed. Mater. Res*, 44, 1999, 446-455.
29. Shabana S, Muzammil MS, Parsana S, Silver nano scaffold formation by flowers of hibiscus rosasinensis". *International journal of herbal medicine*, 1(2), 169-174.
30. Paul S, Jayan A, Sasikumar C S, Cherian SM, Extraction and purification of chitosan from chitin isolated from sea prawn (*fenneropenaeus indicus*). *Asian Journal of Pharmaceutical and Clinical Research*, 7(4), 2014, 201-204.
31. Muzzarelli Raa, *Natural chelating polymers*: Oxford: Pergamon Press, 1973.
32. Yang SF, Leong KF, Du ZH, Chua CK, The design of scaffolds for use in tissue engineering. Part I. Traditional factors. *Tissue Engg*, 6, 2001, 679-689.

33. Gole, A., Dash, C., Ramakrishnan, V., 'Pepsin gold colloid conjugates: preparation, characterization, and enzymatic activity', *Langmuir*, 17, (5), 2001, 1674–1679.
34. Sadhasivam, S., Shanmugam, P., Yun, K.S.: 'Biosynthesis of silver nanoparticles by *Streptomyces hygroscopicus* and antimicrobial activity against medically important pathogenic microorganisms', *Colloid Surf. B*, 81(1), 2010, 358–362.
35. Czechowska-Biskup, Renata, Jarosińska, D, Rokita, Bozena, Ulański, Piotr & Rosiak, Janusz. Determination of degree of deacetylation of chitosan - Comparison of methods. *Progress on Chemistry and Application of Chitin and its Derivatives*. 2012. 5-20.